Available online at www.sciencedirect.com
ScienceDirect
Journal of Nuclear Materials 367–370 (2007) 229–233
journal of nuclear materials
www.elsevier.com/locate/jnucmat

Embrittlement and hardening during thermal aging of high Cr oxide dispersion strengthened alloys

J.S. Lee [a,*], C.H. Jang [b], I.S. Kim [b], A. Kimura [c]

[a] Korea Institute of Nuclear Safety, 19 Guseong-dong, Yuseong-gu, Daejeon 305-338, Republic of Korea
[b] Department of Nuclear and Quantum Engineering, KAIST, 373-1 Guseong-dong, Yuseong-gu, Daejon 305-701, Republic of Korea
[c] Institute of Advanced Energy, Kyoto University, Gokasho, Uji, Kyoto 611-0011, Japan

Abstract

The effects of thermal aging on the microstructure and mechanical property changes in high Cr oxide dispersion strengthened (ODS) steels were investigated by using TEM, microhardness and small punch (SP) tests. The materials used were produced by varying Cr contents from 14 to 22 wt% but keeping yittria contents within 0.36–0.38 wt%. Specimens were thermally aged at temperatures between 430 and 475 °C up to 1000 h. SP-ductile to brittle transition temperature and microhardness of thermally aged ODS steels were significantly increased as a function of Cr contents, aging time and temperature. The main cause of embrittlement is the formation of a Cr-rich α' phase. The hardening appears thermally activated and the apparent activation energy is measured in the range of 214–240 kJ/mol. It is coherent with the activation energy for the diffusion of Cr or Fe in this type of alloys.

1. Introduction

Recent experimental work indicates that the oxide dispersion strengthened (ODS) steels are highly resistant to irradiation embrittlement up to 15 dpa, showing almost no irradiation-induced embrittlement even though some amount of hardening was observed [1]. Furthermore, high Cr ferritic ODS steels with Cr concentrations in the range of 14–22 wt% were recently developed, and they showed high resistance to corrosion in supercritical pressurized water [2] and also to the hydrogen embrittlement such that the critical hydrogen concentration required for a brittle cracking was about one order higher than that for 9Cr reduced activation martensitic steels [3].

Since ODS steels have been developed for the use of high temperature applications in the range from ~400 to 700 °C, they will inevitably experience thermal aging related problems at prolonged service times. It is well known that thermal aging of high Cr ferritic steels can result in the formation of coherent particles of α' (Cr-rich ferrite) with an increase in yield and tensile strength, and a reduction in ductility [4] when in service at temperatures between 400 and 550 °C. This phenomenon, so-called '475 °C embrittlement', is observed in duplex stainless steel and Fe–Cr alloy systems, and it has been extensively studied for Fe–Cr steels [5,6]. However, limited data are available for the microstructural and mechanical

* Corresponding author. Tel.: +82 42 868 0784; fax: +82 42 868 0045.
E-mail address: jslee2@kins.re.kr (J.S. Lee).

0022-3115/$ - see front matter © 2007 Elsevier B.V. All rights reserved.
doi:10.1016/j.jnucmat.2007.03.007

property changes of high Cr ODS steels after thermal aging treatments. In this work, the effects of thermal aging treatment on the microstructural stability and mechanical property changes of ODS steels were investigated by using TEM, microhardness and small punch (SP) tests.

2. Experimental

The materials used were five kinds of ODS steels (K1–K5) produced by varying Cr content from 14 to 22 wt% but keeping yittria contents within 0.36–0.38 wt%. The main chemical compositions of the K1, K2, K3, K4 and K5 steels are 19Cr, 14Cr–4Al, 16Cr–4Al, 19Cr–4Al and 22Cr–4Al, respectively. Detailed chemical compositions of each steel were reported in [2,3]. The microstructures of the steels were examined using transmission electron microscopy (TEM), and thin foils for TEM were fabricated using a twin jet electropolisher in a solution of 10% perchloric acid + 90% ethanol at −30 °C.

Disk type small punch (SP) ($3\phi \times 0.25^{t}$ mm) and tensile specimens (gage = 5 mm, $1.2^{w} \times 0.25^{t}$ mm) were sampled from the extruded rod so that the axis direction is parallel to the transverse and longitudinal direction with respect to the extruded direction, respectively. Tensile properties obtained at room temperature are summarized in Table 1. SP tests were performed at a cross-head speed of 0.2 mm/min. at temperatures from 20 to −196 °C. One millimeter diameter steel balls with Rockwell hardness (HRC) of over 60 were employed for loading fixtures. Specific SP energy was determined by the area under the load–deflection curve per unit thickness of the given specimen, and the SP-ductile to brittle transition temperature (SP-DBTT) was defined as the temperature where the specific SP energy was the average of the maximum specific SP energy and the lower shelf energy. Specimens were thermally aged in a vacuum chamber at temperatures from 430 to 475 °C up to 1000 h. The temperature variation was kept within ±2 °C at the desired aging temperature. Vickers micro-hardness tests were carried out with a 500 g load at room temperature. At least eight measurements were made on each sample.

Table 1
Tensile properties of each ODS steel sampled longitudinal with extruded direction

Index	Yield stress (MPa)	Tensile stress (MPa)	Uniform elongation (%)	Total elongation (%)
K1 (19Cr)	1141.7	1234.5	7	9.6
K2 (14Cr–4Al)	820	936.1	8	13.6
K3 (16Cr–4Al)	811.9	958.9	8.5	13.6
K4 (19Cr–4Al)	853.7	1005.4	9.2	14.2
K5 (22Cr–4Al)	876.4	1024	8.4	14.8

3. Results

3.1. Ductile to brittle transition behavior

SP load–deflection curves as a function of test temperature, before and after aging treatment at 437 °C for 322 h, are shown in Fig. 1. In 14Cr (K2) ODS steel, the maximum SP load increased continuously as the test temperature cooled down to about −100 °C, and decreased abruptly with further cooling. Similar behaviors were also founded in 16Cr (K3) ODS steel. In the case of 19Cr (K4) ODS steel, the maximum SP load tested at room temperature was similar up to about −100 °C, but the specimens broke more earlier than the K2 and K3 ODS, resulting lower absorbed SP energy. Furthermore, when the aging treatment was applied to the K4 ODS, the sample revealed a significantly embrittled nature such that the maximum SP load was greatly reduced at all test conditions, and completely brittle fracture was observed even when tested below −40 °C. However, as Cr content reduced from 19 to 14 w/o, such embrittled behaviors were gradually

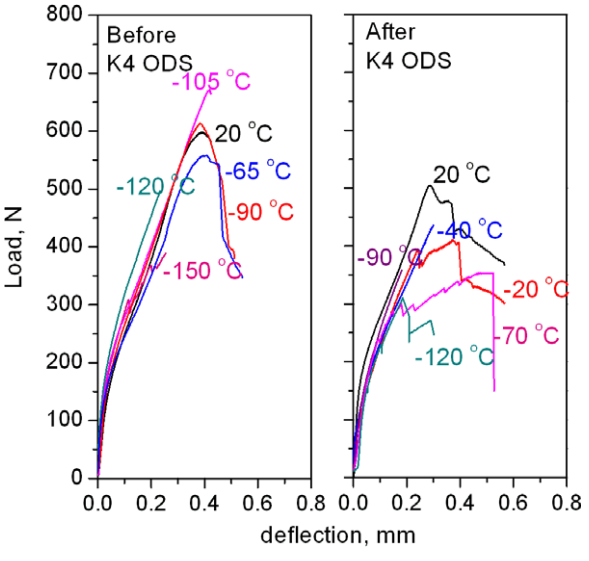

Fig. 1. SP load–deflection curves of 19Cr ODS (K4) steel before and after thermal aging treatment at 437 °C for 322 h.

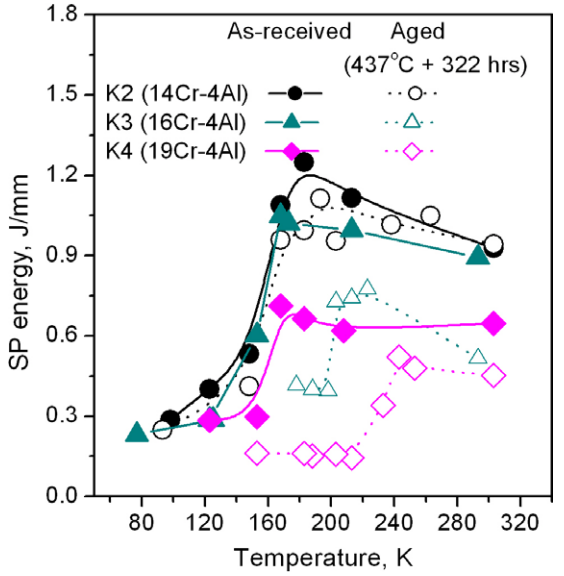

Fig. 2. Effects of thermal aging treatment on the specific SP energy of the ODS steels as a function of test temperature, for samples thermally aged at 437 °C for 322 h.

relieved, showing very weak aging effects on the 14 Cr (K2) ODS steel.

The changes in SP energy by thermal aging are summarized in Fig. 2, showing an increase in SP-DBTT and a reduction in upper shelf energy. In as-received K2, K3 and K4 ODS steel, there was an increase in SP energy with decreasing test temperature up to −110 °C, and a drop in SP energy was observed by further cooling. The SP-DBTT was around −120 °C, irrespective of the ODS materials. On the other hand, when thermal aging treatment was applied at 437 °C for 322 h, the degree of embrittlement increased with Cr content such that the increase in SP-DBTT associated with the reduction in upper shelf energy is 10, 50 and 73 °C in 14 Cr (K2), 16Cr (K3) and 19Cr (K4) ODS steel, respectively.

3.2. Vickers micro-hardness measurement

The hardening amount of each ODS steel due to thermal aging treatment at 475 °C is presented in Fig. 3. As aging time increased up to 1000 h, the hardness value increased exponentially for all the materials, Fig. 3(a). At the same time, when Cr content increased from 14 to 22 w/o, the hardness increases, respectively from 30 to 110. However, K1 ODS steel (19 Cr without Al addition) showed the highest hardness values, the ΔH_v in K1 and K4 ODS (19Cr with 4Al) are almost the same at a given test condition, suggesting there is no effect of Al addition on the thermal aging induced-hardening.

Hardening behaviors of ODS steels as a function of aging parameter, P, were plotted in Fig. 3(b). Here, P is the Larson–Muller parameter divided by a factor of one thousand, $P = T(20 + \log t)10^{-3}$. From the figure, the ΔH_v in each ODS steel revealed a linear relationship with the aging parameter, P. Furthermore, as the Cr content increased, the amount of hardening also increased linearly as well.

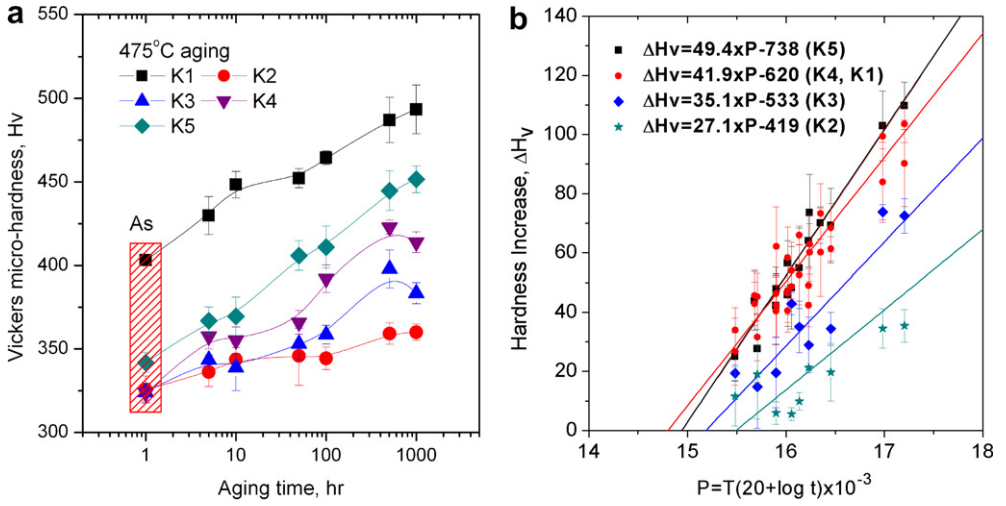

Fig. 3. (a) Vickers micro-hardness (H_v) as a function of the aging time in each ODS steel, thermally aged at 475 °C and (b) increase in Vickers micro-hardness (ΔH_v) as a function of aging parameter P, $P = T(20 + \log t)10^{-3}$, where T is the temperature and t is the aging time.

From these results, we could obtain the generalized hardening formula as a function of Cr, aging temperature and time as follows:

$$\Delta H_v = (2.37\mathrm{Cr} - 3.02) \times T(20 + \log t) \times 10^{-3} - (34.8\mathrm{Cr} - 31.5),$$

where T is the aging temperature [K] ($703 \leqslant T \leqslant 748$), t is the aging time [hour] ($5 \leqslant t \leqslant 1000$), and Cr is the weight percent of Cr ($14 \leqslant \mathrm{Cr} \leqslant 22$).

3.3. Microstructural features

Gradual microstructural changes were identified, depending on the aging time, when samples were thermally aged at 475 °C. Fig. 4 shows the formation of a two-phase modulated structure (gray and white) in the ferrite matrix as aging time increased. Based on the EDS line scanning element profiles, we could know that it resulted from the formation of Cr-enriched and separate Fe-enriched zone.

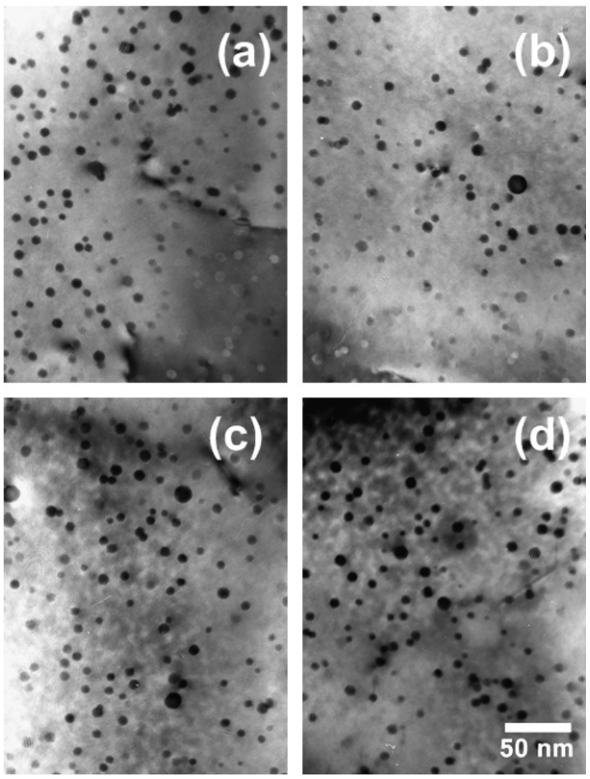

Fig. 4. Transmission electron micrographs, showing a thermally aged 22Cr (K5) ODS steel at temperature 475 °C up to (a) 5, (b) 50, (c) 505 and (d) 1000 h, respectively, black dots = oxide particles, bright field images.

But, the current aging conditions did not result in any changes of the number density and size of the oxide particles. The average diameter and number density of oxide particles in K1 ODS steel were measured as 2.4 nm and $1.4 \times 10^{23}\ \mathrm{m}^{-3}$, respectively. However, when 4% Al was added, the size and number density of the particles changed from 2.4 to 6–7 nm and from 1.4×10^{23} to $1\text{–}2 \times 10^{22}\ \mathrm{m}^{-3}$. On the other hand, after thermal aging treatment at 437 °C for 322 h, no discernable precipitation could be found in any ODS steel even though they exhibit significant embrittlement accompanied by hardening.

4. Discussion

4.1. Effects of Cr and Al element

TEM investigation reveals that the phase separation of ferrite phase into Cr-enriched and Fe-enriched phases in ODS steels is similar to that observed in Fe–Cr and many Fe–Cr–X systems which experience spinodal decomposition within a miscibility gap under certain conditions. Spinodal decomposition is related to the up-hill diffusion process of Cr, which means the diffusion activation energy of Cr will not be affected much by the changing Cr content in the high Cr ferritic ODS steel matrix, and within the miscibility gap, Cr content will control the total amount of α' phase by its lever rule. These facts were confirmed by measurement of the activation energy. Since the hardening is thermally activated, the apparent activation energy is measured assuming the Arrhenius type rate equation. Fig. 5 presents the activation energy determined by micro-hardness data, showing that the energy is in the range of 214–240 kJ/mol and the variation of the activation energy between the ODS steels is not significant. Furthermore, this energy is very similar to the diffusion activation energy of Cr (203 kJ/mol) and Fe (211 kJ/mol) in Fe–26Cr steel [7], therefore, the formation of the Cr-rich α' phase is related to the diffusion of Cr and/or Fe in the ferrite matrix. Also, there was no effect of Al addition on the total amount of hardening. The hardening amount in 19Cr ODS steels with (K4) and without Al addition (K1) is almost the same at a given test condition, and the EDS line scanning results do not reveal any partitioning of Al element into α and α' phase under the current test conditions.

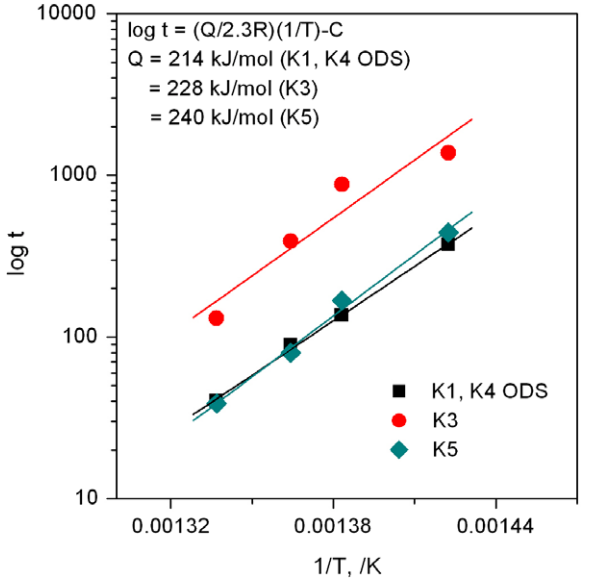

Fig. 5. Activation energy of each ODS steel determined by micro-hardness data based on Arrhenius type rate equation.

4.2. Embrittlement mechanisms

The presence of Cr-enriched α′ phase is fully responsible for the hardening and its resultant embrittlement of thermally aged high Cr ODS steels. α′ phase results in the increase in internal stress, which in turn evokes the hardening of materials by hindering the dislocation movement. According to Park et al. [8], such an increase in internal stress is caused by the atomic misfit and a different modulus for the α and α′ phases, and it is directly proportional to the amount of composition fluctuation. This increased stress raises the critical resolved shear stress for slip, thus increasing the probability of forming a $\{1\,1\,2\}\langle 1\,1\,1\rangle$ twin over generating slip in the bcc ferrite matrix [9]. But, in the current TEM observations, we could not ascertain the creation of deformation twins on the significantly hardened SP specimens, but we simply observe the dislocation cell structure with the presence of Orowan loops. Based on the results, the occurrence of α′ phase in ODS steels retards the motion of dislocations and hardens the materials, which results in the loss of toughness and the ductile to brittle transition temperature shift.

5. Conclusions

After thermal aging treatments at temperatures from 430 to 475 °C, significant embrittlement associated with hardening was observed in high Cr ODS steels. The degree of embrittlement increases with Cr content such that when thermally aged at 437 °C for 322 h, the increases in SP-DBTT are about 10, 50 and 73 °C in 14, 16 and 19 Cr ODS steel, respectively. Furthermore, the hardening relationship can be obtained successfully as a function of Cr content and aging time. Based on the TEM investigations, the main cause of embrittlement is the formation of Cr-rich coherent ferrite phase, α′ phase. The apparent activation energy of thermally activated hardening is measured in the range of 214–240 kJ/mol, which is similar to the diffusion activation energy of Fe and Cr in alpha iron. Considering the aging embrittlement phenomena in high Cr ODS steels, 14 Cr ODS steel is considered to be a more promising material than the others at service temperatures.

Acknowledgements

This work was partially supported by the Ministry of Science and Technology of Korea through the HANARO Utilization Program, which is one of the National Nuclear R&D Programs (2005).

References

[1] T. Yoshitake, T. Ohmori, S. Miyakawa, J. Nucl. Mater. 307–311 (2002) 788.
[2] H.S. Cho, A. Kimura, S. Ukai, M. Fujiwara, J. Nucl. Mater. 329–333 (2004) 387.
[3] J.S. Lee, A. Kimura, S. Ukai, M. Fujiwara, J. Nucl. Mater. 329–333 (2004) 1122.
[4] R.L. Klueh, D.R. Harries, ASTM (2001) 39.
[5] M.H. Mathon, Y. de Carlan, G. Geoffroy, X. Averty, A. Alamo, C.H. de Novion, J. Nucl. Mater. 312 (2003) 236.
[6] F. Bley, Acta Metall. Mater. 40 (1992) 1505.
[7] E.A. Browdes, G.B. Brook (Eds.), Smitells Metals Book, Seventh ed., Butterworth, Heinemann, 1992, p. 13.
[8] K.H. Park, J.C. Lasalle, L.H. Schwartz, M. Kato, Acta Metall. 34 (9) (1986) 1853.
[9] T.J. Nichol, A. Datta, G. Aggen, Metall. Trans. A 11A (1980) 573.